Wideband Compact Antenna with Partially Radiating Coplanar Ground Plane

Ahmed Toaha Mobashsher[1], Mohammad Tariqul Islam[1], and Norbahiah Misran[2]

[1] Institute of Space Science (ANGKASA)
Universiti Kebangsaan Malaysia, Bangi, Selangor, Malaysia
i_toaha@yahoo.com, tariqul@ukm.my

[2] Dept. of Electrical, Electronic, and Systems Engineering
Universiti Kebangsaan Malaysia, Bangi, Selangor, Malaysia
bahiah@vlsi.eng.ukm.my

Abstract ─ Many of today's portable communication applications require antennas that are compact, broadband, and easily integrable in a big variety of terminal geometries. This paper presents a compact wideband antenna with partially radiating coplanar ground plane. The prototype of the antenna shows a wide bandwidth (VSWR ≤ 2) of 92% (from 3.53GHz to 9.5GHz). The antenna also exhibits maximum gain of 3.5*dBi* and stable radiation patterns over the whole bandwidth. Nevertheless, in this paper the significance of the ground planes on the operating bandwidth are examined with the help of current distribution and discussed in detail with supporting parametric analysis.

Index Terms ─ Coplanar waveguide feeding, radiating ground plane, wideband antenna.

I. INTRODUCTION

Over the past decade, extensive research on broadband antennas, with low-profile, lightweight, flush mounted, and single-feed to fit the limited equipment space of the portable wireless devices, has contributed to the development of modern communication technology [1]. Wideband antennas play a key role in the faithful operation of these evolving high data rate transceivers. While the bandwidth of antennas is desired to be increased drastically, the size has to be decreased correspondingly due to the demands of portable devices. Nevertheless, polarization, radiation patterns and gains are also important factors in the application of antennas in contemporary and future broadband wireless communication systems.

In order to recover these obstructions, development, and application of cutting-edge technologies are needed that can facilitate compact broadband antennas that can be manufactured and integrated into the portable devices to provide highly survivable, yet lightweight and reliable systems. Because of the attractive features of thickness, weight, efficiency, conformability and simplicity of manufacture, microstrip antennas are widely implemented in many applications, especially in wireless communication. However, narrow bandwidth is the main limitation that restricts the scope of microstrip patch antenna technology.

The new co planar waveguide structure, used for printed antennas to attain wide bandwidth has recently attracted huge attention. Numerous advantages have been obtained by feeding a radiating element with coplanar waveguide (CPW) feeds. When compared with other printed radiating elements, CPW-fed antennas possess advantages of not only a broad bandwidth, but also a smaller mutual coupling between adjacent lines [2]. Another advantage of coplanar fed antenna is lower radiation leakage and less dispersion than microstrip lines. Moreover, this feed design eliminates the competition for surface space between the antenna elements and the feed network. Owing to the uniplanar design, with coplanar waveguide the integration capability with

solid-state active and passive components is easier, since these components can be fabricated on one side of the planar substrate, eliminating the need for via hole connections. In response to the increasing demand for compact, broadband, and easily fabricated antennas for use in various wireless communication systems, several CPW-fed printed antennas have been developed over the past decade [3–9]. However, these antennas either have inconvenient shape or difficult to fabricate, which demands miniaturized simple antennas.

In this paper, a simple and compact antenna is introduced with a wideband characteristic impedance bandwidth. The antenna consists of a coplanar waveguide fed radiating patch and two coplanar ground planes. The ground planes partially radiate and responsible for achieving a wide bandwidth with a small structure. The effect of the ground planes on the operating bandwidth are investigated with the help of current distribution and discussed in detail with supporting parametric analysis. A prototype has been fabricated and the measured results are also presented.

II. ANTENNA CONFIGURATION

The geometry of the proposed CPW-fed planar antenna for wideband operations is shown in Fig. 1. For the design studied here, the antenna is etched on the same side of a low cost FR4 substrate with the dielectric constant, ε_r of 4.6 and the substrate thickness, h of 1.6mm, while the other side is without any metallization. A CPW transmission line, which consists of a metal strip thickness of W_{f1} and a gap distance of d between the single strip and the coplanar ground plane, is used for feeding the antenna. It is important to note that here W_{f1} corresponds to 50Ω CPW feed line.

The ground planes are unsymmetrical to each other. On the right side an inverted L-shaped ground plan is positioned, which comprises an overlapped vertical and horizontal sections with dimension of $W_{r1}\times L_{r1}$ and $t_{r1}\times L_{r2}$. These two parts are overlapped on an area of $t_{r1}\times L_{r1}$. However, on the left side a U-shaped ground plane is used to attain the lower frequencies of the broadband antenna. The U-shaped ground has a length of L_{l2} and the dimensions of upper and lower arm are $W_{l2}\times t_{l2}$ and $(W_{l1}-t_{l1})\times L_{l1}$, respectively.

The basis of the antenna structure is of vertical bow-tie shaped with unequal wings. The total length of the radiating element is L_{f2}. The tapered transition for the lower wing is L_{f3}, which is W_{f2} wide at that position. On the other hand, the length of upper wing is L_{f4} and final breadth is W_{f3}. The lower wing connected at the end of the L_{f2} long CPW feed line.

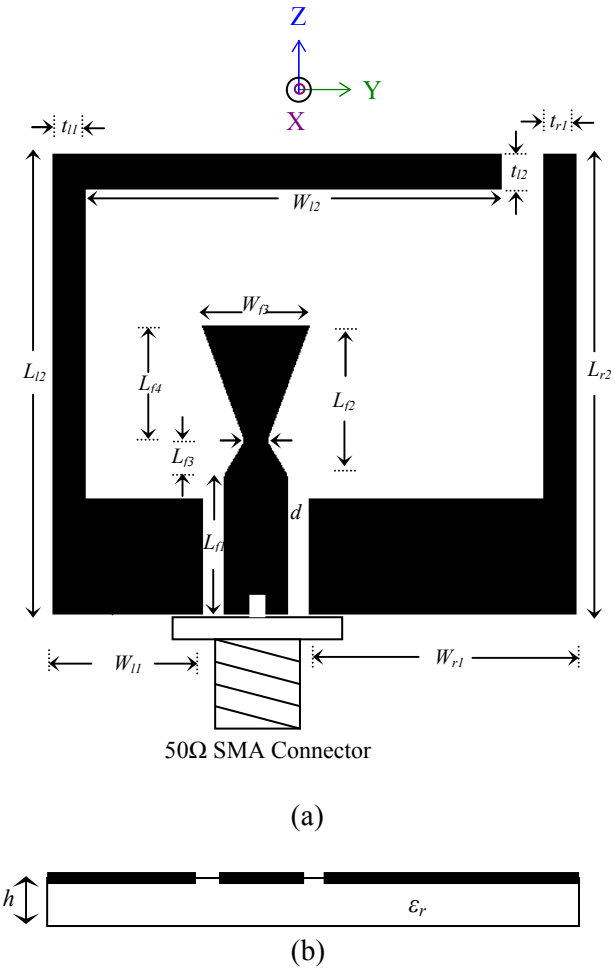

Fig. 1. Schematic diagram of the antenna a) top view, b) side view.

Table 1: Design geometrical parameters of the proposed antenna

Parameters	***Value in* mm**
{W_{f1}, L_{f1}}	*{3, 6}*
{ W_{f2}, W_{f3}, L_{f2}, L_{f3}, L_{f4}}	*{1, 5, 6.5, 1.5,5}*
{ W_{l1}, W_{l2}, L_{l1}, L_{l2}, t_{l1}, t_{l2}}	*{7, 19.5, 5, 20, 1.5, 1.5}*
{ W_{r1}, L_{r1}, L_{r2}, t_{r1},}	*{12.5, 5, 20, 1.5}*

To investigate the performance of the proposed antenna configurations in terms of

achieving the wideband operations a commercially available full-wave, method-of-moment code based electromagnetic simulator Zeland IE3D version 12 [10], was used for required numerical analysis and obtaining the proper geometry parameters in Fig. 1, and then the optimal dimensions were determined from experiments. The details of various parameters of the antenna printed on FR4 substrate are listed in Table 1 for better convenience.

III. INVESTIGATION & ANALYSIS

In this section, the effects of the proposed slot antenna parameters are discussed and analyzed using IE3D software, to facilitate more elaboration of the design and optimization processes for readers. Primarily, with the help of the current distribution, the analysis has been carried out to investigate the partial radiation of the antenna coplanar ground planes. At the same time, to derive some mathematical equations corresponding to the current paths of resonant frequencies within the wide bandwidth. The analysis covers the influences of varying the lengths and width of the arms of the inverted L-shaped right ground and U-shaped right ground plane on VSWR, the implication of choosing the shape of vertical-bow-tie patch for the design and selecting the size of the feeding line for achieving the best performance of wide bandwidth. For better convenience of the effect on the performance of the antenna upon changing the parameters, only one parameter is changed at a time, while keeping others unchanged.

A. Current distribution

The excited surface current distributions, obtained from the IE3D simulation, on the radiating edges of the proposed antenna at the four resonant frequencies, namely 3.59GHz, 4.35GHz, 6GHz, and 8.45GHz, respectively, are presented in Figs. 2 and 3. Arrows show the direction of the current direction and the darker color shows the current intensity on that area of the antenna, while the blue color region shows the null current at that portion. As expected, four dominating current paths have been found, which primarily cause of four resonant modes. These four resonances adding side by side with each other form the broad impedance bandwidth. The path equations at each resonance are tabulated in Table 2. These equations provide the some basic information about the dependencies of resonant frequencies upon various dimensions of the antenna.

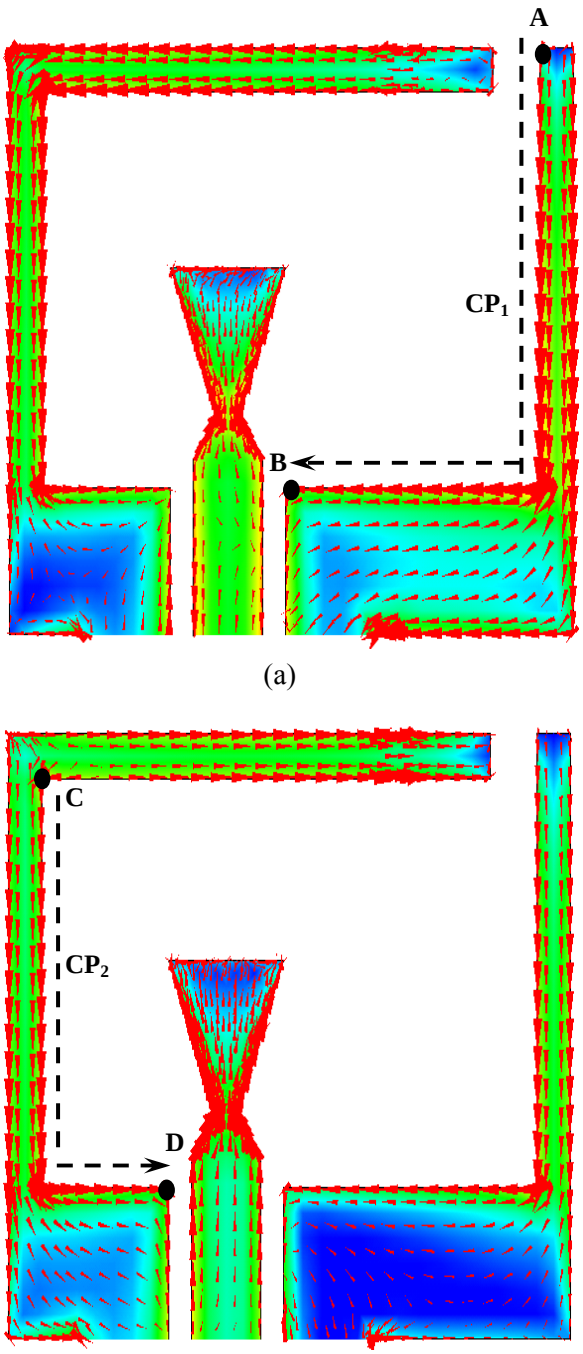

Fig. 2. Surface current distribution of the proposed antenna a) 3.59GHz, b) 4.35GHz.

At f = 3.59GHz, the current around inner edge of the right ground plane of the CPW antenna is stronger than other areas. But current direction at f

= 4.35GHz is more concentrated in the lower inner side of the left ground plane. The third resonance is particularly due to the monopole like behavior of the CPW-fed radiating element. The current path clearly observed by the intensity of current components and marked as CP_3 in Fig. 3(a). On the other hand, the forth resonance of the antenna is due to the dipole like behavior of the left U-shaped ground plan. The dominating current path is denoted by CP_3 and marked by a black dotted line in Fig. 3(b). It is noted from Table 3 that in both of the first two resonant points the current paths corresponds to a length which is slightly longer than one-quarter wavelength of the respective operating frequencies. And for the forth resonant it is also marginally longer than the one-half wavelength of the respective frequency. These deviations can be attributed to the additional effect of the loading of the particular resonant part by the remaining non-resonant part of the whole structure.

Table 2: Information derived from the current distribution analysis

Resonance Number	Path Equation
1	$CP_1 = L_{r2} - L_{r1} + W_{r1} - t_{r1}$
2	$CP_2 = L_{l2} - L_{l1} - t_{l2} + W_{l1} - t_{l1}$
3	$CP_3 = L_{f1} + \sqrt{L_{f3}^2 + \{(W_{f1} - W_{f2})/2\}^2} + \sqrt{L_{f4}^2 + \{(W_{f3} - W_{f2})/2\}^2} + W_{f3}/4$
4	$CP_4 = L_{l2} - L_{l1} + W_{l1} - t_{l1}$

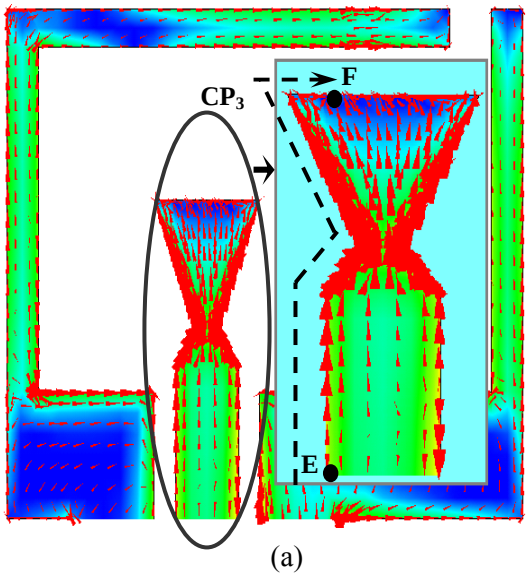

(a)

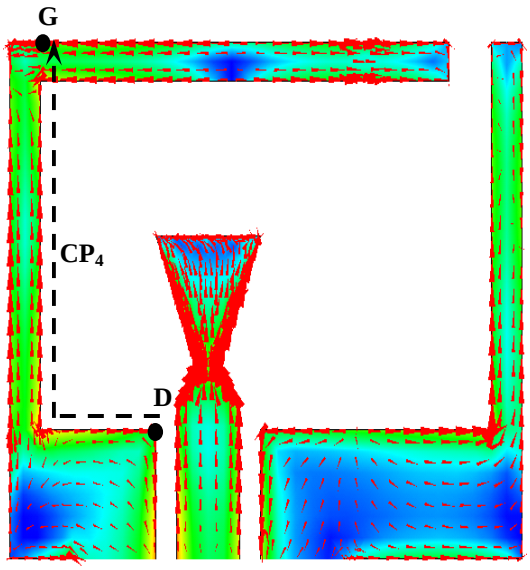

(b)

Fig. 3. Surface current distribution of the proposed antenna a) 6GHz, b) 8.45GHz.

Table 3: Current path relative to free space wavelength (λ_o)

Resonance Number	Resonant Point	Current Path	Relative to free space wavelength (λ_o) at respective resonance
1	3.59GHz	CP_1 (A-B)	0.311 λ_o
2	4.35GHz	CP_2 (C-D)	0.275 λ_o
3	6GHz	CP_3 (E-F)	0.244 λ_o
4	8.45GHz	CP_4 (D-G)	0.577 λ_o

B. Dependence on length of right ground plane L_{r2}

In order to examine the sensitivity of L_{r2} on the first resonance frequency pointed out in the preceding section, a parametric analysis has been done. The results are presented in Fig. 4. As predicted, the increment of L_{r2} decreases the first resonance, while have some effects on the impedance matching on other resonant point. It is important to observe that upto L_{r2}=15mm the first and second resonances coincided and could not be noted separately from each other. However, as L_{r2} increases to 20mm the current path increased and the first resonance is cleared out.

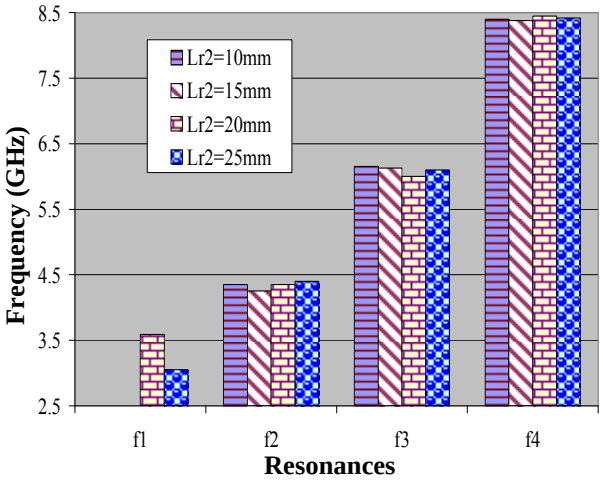

Fig. 4. Effect on resonant frequencies due to change of L_{r2}.

C. Dependence on lower arm length of left U-shaped ground plane L_{l1}

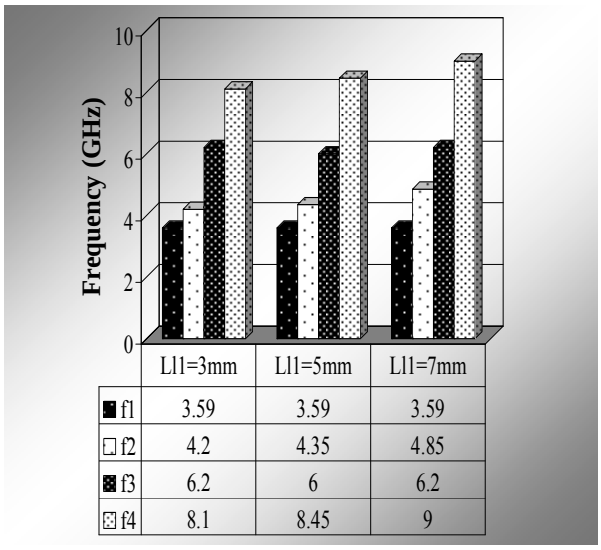

Fig. 5. Effect on resonant frequencies due to change of L_{l1}.

Figure 5 projects the effect of changing L_{l1} on the resonances. As discussed previously, the length of L_{l1} mainly influences the second (f2) and forth resonance (f4). As seen from the plot, both of the resonant frequencies tend to increase as L_{l1} is increased from 3 to 7mm. This is also justified by the mathematical expression of CP2 and CP4 mentioned in Table 2. This may be a way to increase the overall bandwidth of the antenna. Although the increment of resonances reduces the impedance matching, it makes discontinuity in the operating bandwidth.

D. Dependence on CPW-fed radiation element parameters W_{f2} & W_{f3}

The mathematical equation for the third current path, CP3 leads us to the effect of changing W_{f2} and W_{f3}, which is verified by the parametric study on both of these parameters shown in Fig. 6, keeping all others the same. The value of W_{f2} is increased from 0.5mm up to 5mm and the third resonant point increases from 5.85 to 6.43GHz. The contradictorily increment of W_{f3} decreases the third resonant point. However, the change of these parameters also has some additional effect on other resonances, but they are mainly due to the loading mismatch.

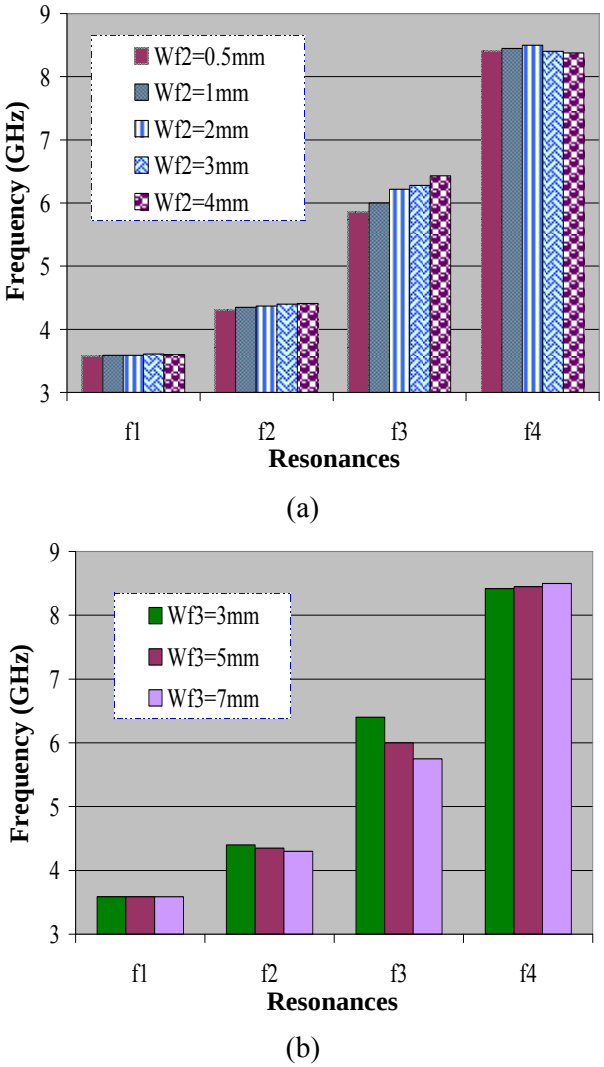

Fig. 6. Effect on resonant frequencies due to change of (a) W_{f2} and (b) W_{f3}.

E. Dependence on coupling gap d between the feed line and ground plane

Additionally, an important feature of the proposed antenna is the influence of impedance matching caused from the coupling effects between the feed line and the coplanar ground plane over the whole operating band, especially over the first and forth resonances. For this, the effect of the gap distance d on the performance of the proposed antenna was also studied and presented in Fig. 7. The obtained results indicate that the VSWR increases and consequently the bandwidth of the antenna are reduced with increasing distance of *d*. The first and forth antenna resonances tend to rise to higher frequencies with the increase in VSWR while the third resonance decreases to lower frequency. However, the second resonance seems to have no effect upon changing the coupling gap between the feed line and ground plane.

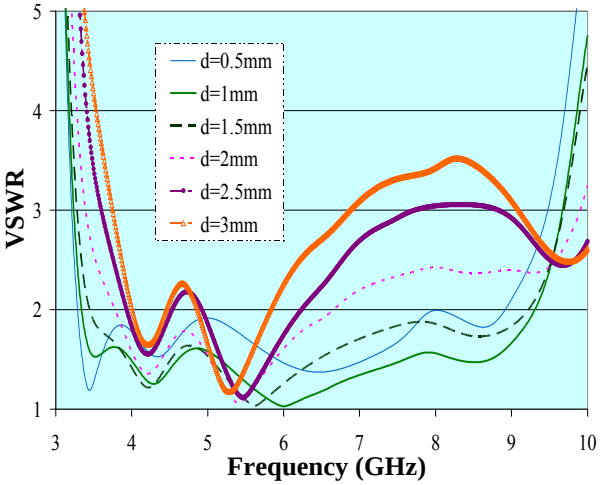

Fig. 7. Effect on resonant frequencies due to change of *d*.

IV. RESULTS AND DISCUSSIONS

The proposed coplanar fed broadband antenna has been prototyped for the verification and measured using Agilent E9362C network analyzer. It was seen that the measured results agrees the simulated results. The prototypes are shown in Fig. 8.

The measured and simulated voltage standing wave ratios (VSWR) of the proposed antenna (denoted by a solid and dashed line, respectively) are depicted in Fig. 9. The measured VSWR curve shows that the proposed antenna produces a total bandwidth of 5.97GHz ranging from 3.53GHz to 9.5GHz below VSWR $\leq$ 2, which is equivalent to 92% impedance bandwidth centered at 5.52GHz. Nevertheless, the simulated VSWR graph shows a bandwidth of 5.99GHz (94.5%, 2 $\geq$ VSWR) from 3.34GHz to 9.33GHz. The slight difference of the simulated and measured results can be attributed to the fabrication and measurement limitations.

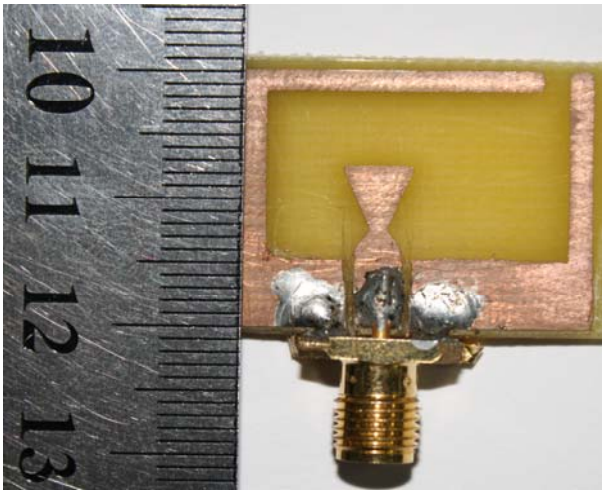

Fig. 8. Photograph of the fabricated prototype of the proposed wideband antenna.

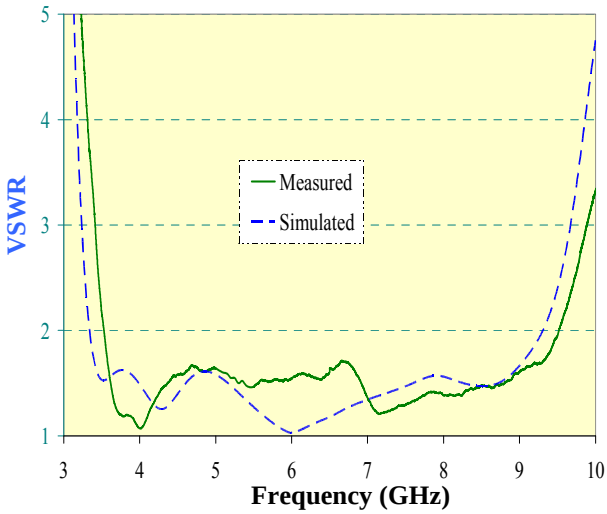

Fig. 9. Simulated and measured VSWR of the proposed wideband antenna.

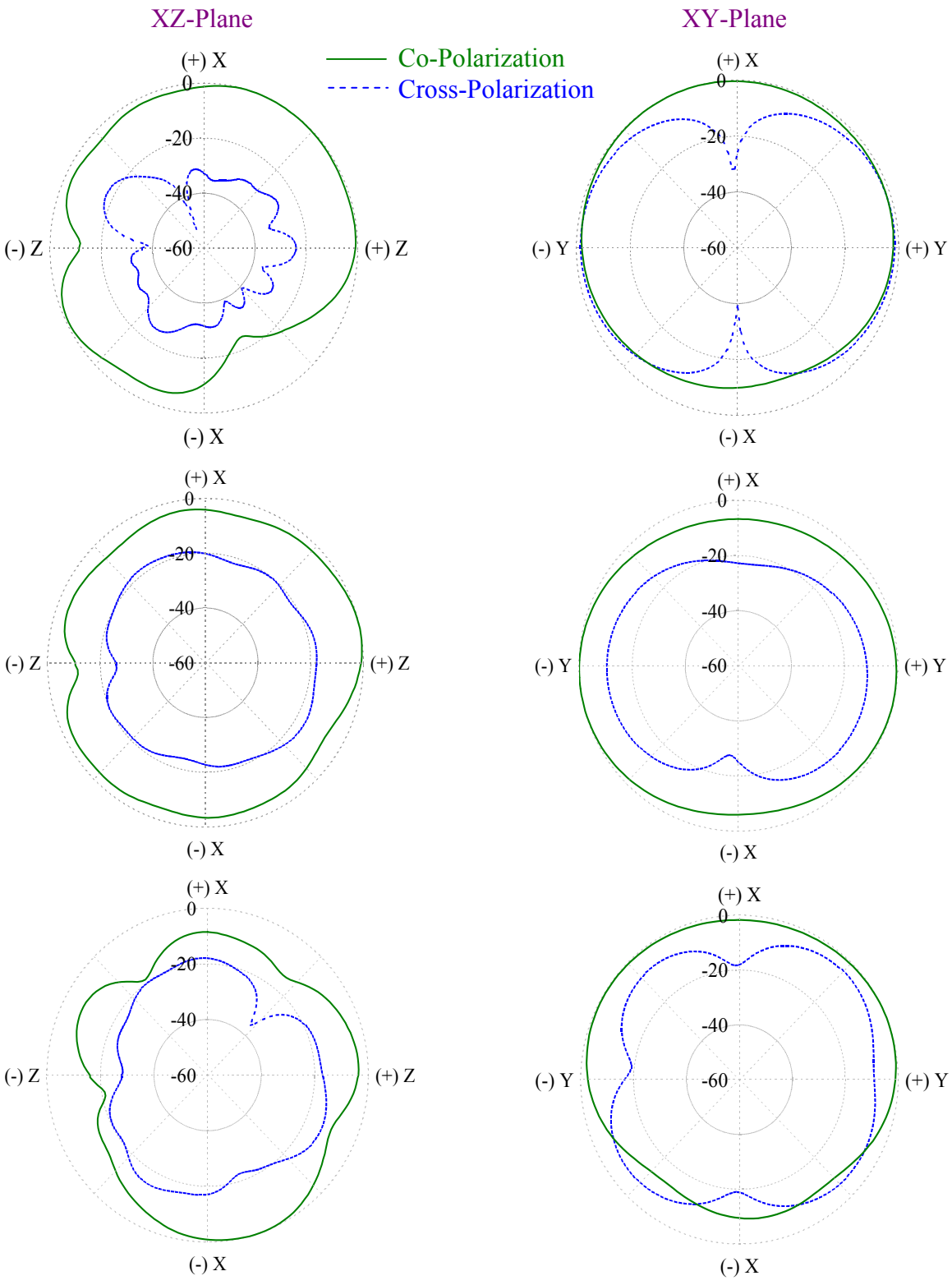

Fig. 10. Radiation pattern (XZ & XY-plane) of the proposed antenna at 4GHz, 6GHz, and 8.4GHz.

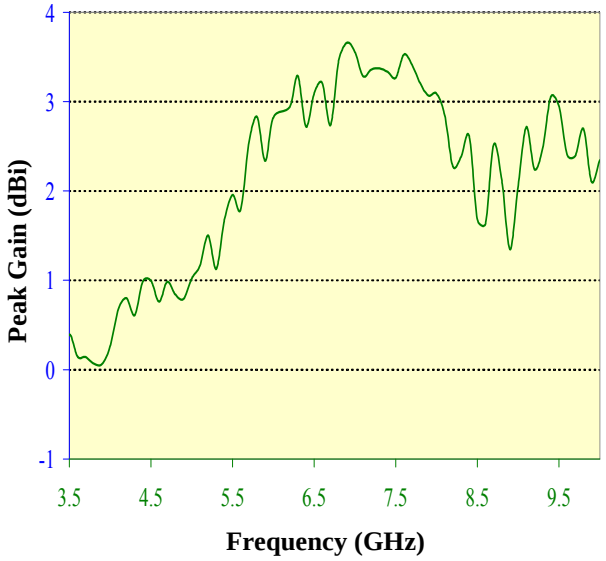

(a)

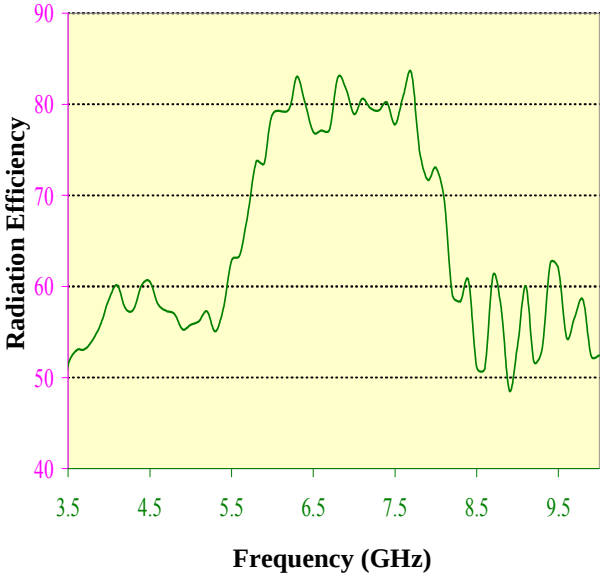

(b)

Fig. 11. Measured (a) gain and (b) radiation efficiency of the designed antenna.

The measured E (XZ) and H (XY) plane radiation patterns of the proposed antenna at 4GHz, 6GHz, and 8.4GHz have been shown in Fig. 10. It can be seen that the designed antenna produce a nearly omni directional radiation pattern. In spite of the slight unsymmetrical structure of the antenna, an almost symmetrical radiation pattern with no back lobe radiation has been observed. One of the significant advantages of a symmetrical radiation pattern is that the maximum power direction would always be at the broadside direction and would not shift to different directions at different frequencies. Consequently, the antenna shows a broad half power beam width (HPBW) of almost ± 80, ± 85, and ± 65 degrees in the E-plane as well as ± 140, ± 95, and ± 100 degrees in the H-plane at the frequencies of 4GHz, 6GHz, and 8.4GHz, respectively. However, it was realized that the cross polarization level for the antenna is higher at low frequency, 4GHz, which is also a degenerative effect of compact antennas. For compact antennas, the ratio of width and height increases, which results in a greater surface wave to produce diffraction at the dielectric's edge, thus contributing to higher cross-polarization levels [11]. However in the higher frequencies, the cross polarization goes lower, as the respective size of the antenna increases with the decrease in wavelength for higher frequencies.

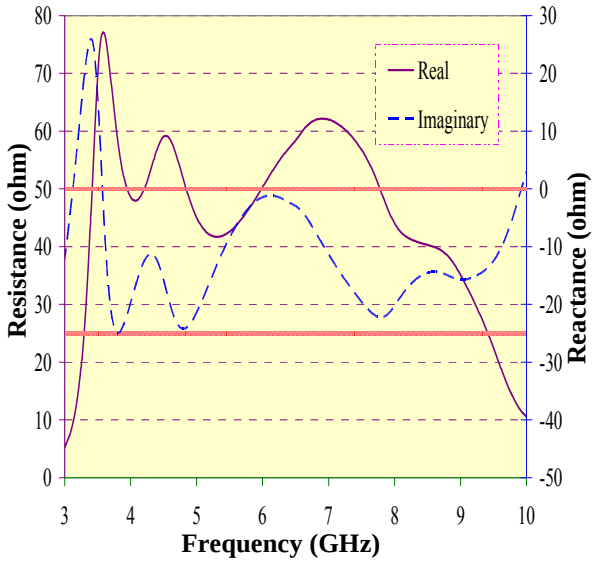

Fig. 12. Simulated input impedance of the proposed wideband antenna.

Figure 11(a) illustrates the measured maximum antenna gain for frequencies over the whole operating band. The antenna exhibits an overall gain of more than 0*dBi,* with a gain variation of about 3*dBi* within the entire bandwidth. The peak gain of 3.5*dBi* is attained at near 7GHz. The gain variation of the antenna can be attributed to the copper loss of the antenna

which was not taken into account in the simulation and also the loss due to the SMA connector of the antenna. The radiation efficiency of the antenna is depicted in Fig. 11(b). Regardless of the high loss ($\tan\delta = 0.02$) of the FR4 substrate, the antenna shows a minimum efficiency of 50%. It is suggested to use low loss Duroid substrate to increase the radiation efficiency and gain of the proposed antenna. But in that case, the cost of the antenna would increase. That's what this phenomenon in not premised.

The antenna input impedance plotted in Fig. 12 displays four good quality factor resonances within the frequency band of interest which allows a wide band impedance matching. The resonances are identified as local maxima of the impedance imaginary part. The antenna shows low matching in the first resonance, which can be caused by the inductive peak of the imaginary curve. However, this peak in the inductive region is also responsible for the good radiation efficiency at the first resonance point shown in Fig. 11(b). Other than the first resonance, the capacitive behavior of the antenna prevents the imaginary part from crossing zero, particularly for good quality factor resonances [12]. The real part of input impedance literally swings around the 50Ω line over the entire bandwidth of the antenna. It is interesting to note that when the real part of input impedance falls below 25Ω the antenna voltage standing wave ratio goes over 2. So in a way, the whole bandwidth (VSWR ≤ 2) can also be defined by the 25Ω line of the real input impedance curve.

IV. CONCLUSION

A printed 50Ω fed antenna for wireless communications has been presented. The proposed antenna with two unsymmetrical coplanar ground elements, namely inverted-L and U-shaped ground provides a wideband operation easily covering 5.97GHz from 3.53GHz to 9.5GHz. The effect of the partial radiating ground plane has been analyzed pointing out the mathematical expression of the current path from the simulated current distribution and was verified by means of the parametric analysis. Besides its wideband characteristics, the proposed antenna remains compact and possesses maximum 3.5*dBi* gain with good radiation patterns, making it a good candidate for wireless communication applications.

ACKNOWLEDGMENT

The authors would like to thank the Institute of Space Science (ANGKASA) of Universiti Kebangsaan Malaysia (National University of Malaysia).

REFERENCES

[1] W.-C. Liu and J.-K. Chen, "A Dual-Band CPW-Fed Monopole Antenna for IMT-2000/WLAN," *Microwave Journal*, vol. 53, no. 5, pp.124-134, 2010.

[2] R. B. Hwang, "A Broadband CPW-Fed T-Shaped Antenna for Wireless Communications," *IEE Proc. - Microwave Antennas Propagations*, vol. 151, no. 6, pp. 537-543, 2004.

[3] J. William and R. Nakkeeran, "A Novel Compact CPW-Fed Wideband Slot Antenna," *3rd European Conference on Antennas and Propagation*, pp. 147-1474, 2009.

[4] A. U. Bhobe, C. L. Holloway, M. Piket, and R. Hall, "Wide-Band Slot Antennas with CPW Feed Lines: Hybrid and Log-Periodic Designs," *IEEE Transactions on Antennas and Propagation*, vol. 52, no. 10, pp. 2545-2554, 2004.

[5] Nasimuddin and Z. N. Chen, "Wideband Multilayered Microstrip Antennas Fed by Coplanar Waveguide-Loop with and without Via Combinations," *IET Microwave Antennas Propagations*, vol. 3, no. 1, pp. 85-91, 2009.

[6] A. A. Eldek, A. Z. Elsherbeni, C. E. Smith, and K. F. Lee "Wideband Planar Slot Antennas," *Applied Computational Electromagnetic Society (ACES)* Newsletter, vol. 19, no. 1, pp. 35-48, 2004.

[7] R. H. Patnam, "Broadband CPW-Fed Planar Koch Fractal Loop Antenna," *IEEE Antennas and Wireless Propagation Letters*, vol. 7, pp. 429-431, 2008.

[8] K. Han, Y. Park, H. Choo, and I. Park, "Broadband CPS-Fed Yagi-Uda Antenna," *Electronics Letters*, vol. 45, no. 24, pp. 1207-1209, 2009.

[9] T. N. Chang and G. A. Tsai, "A Wideband Coplanar Waveguide-Fed Circularly Polarised Antenna," *IET Microwave Antennas Propagations*, vol. 2, no. 4, pp. 343-347, 2008.

[10] IE3D version 12, 2010. California: Zeland Software Inc.

[11] I-F. Chen and C.-M. Peng, "A Novel Reduced Size Edge-Shorted Patch Antenna for UHF Band Applications," *IEEE Antennas and Wireless Propagation Letters*, vol. 8, pp. 475-477, 2009.

[12] F. Demeestere, C. Delafield, and J. Keignart, "A Compact UWB Antenna with a Wide Band Circuit Model and a Time Domain Characterization," *IEEE International Conference on Ultra-Wideband*, pp. 345-350, 2006.